Colloids and Surfaces A: Physicochem. Eng. Aspects 448 (2014) 9–15

Contents lists available at ScienceDirect

Colloids and Surfaces A: Physicochemical and Engineering Aspects

journal homepage: www.elsevier.com/locate/colsurfa

Characterization of liposomes and silica nanoparticles using resistive pulse method

Yauheni Rudzevich[a], Yuqing Lin[a], Adam Wearne[a], Antonio Ordonez[a], Oleg Lupan[a,b], Lee Chow[a,*]

[a] Department of Physics, University of Central Florida, Orlando, FL 32816, USA
[b] Department of Microelectronics and Semiconductor Devices, Technical University of Moldova, 168 Stefan cel Mare Blvd., Chisinau, MD-2004, Republic of Moldova

HIGHLIGHTS

- New technique for simultaneous nanoparticles size and velocity measurements is proposed.
- Show size distribution of 40 nm and 90 nm in radius SiO_2 nanoparticles and 40 nm liposomes.
- Measurements of electrophoretic velocity of 40 nm and 90 nm SiO_2 nanoparticles presented.
- Different particles concentrations were examined.

GRAPHICAL ABSTRACT

We demonstrated a novel approach to simultaneously measure electrophoretic velocity and size distribution of organic and inorganic colloids in a size range 40–200 nm. This precise and accessible, single particle resolution technique is a promising alternative to dynamic light scattering and laser doppler velocimetry.

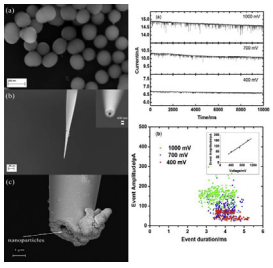

ARTICLE INFO

Article history:
Received 11 November 2013
Received in revised form 17 January 2014
Accepted 31 January 2014
Available online 13 February 2014

Keywords:
Nanoparticles
Electrophoresis
Nanopores
Liposomes
Translocations
Nanopipette

ABSTRACT

The ability to precisely count inorganic and organic nanoparticles and to measure their size distribution plays a major role in various applications such as drug delivery, nanoparticles counting, and many others. Here we employ a simple resistive pulse method that allows translocations, counting, and measuring size and velocity distribution of silica nanoparticles and liposomes with diameters from 50 nm to 250 nm. This technique is based on the Coulter counter technique but has nanometer size pores. It was found that ionic current drops when nanoparticles enter the nanopore of a pulled micropipette, producing a clear translocation signal. Pulled borosilicate micropipettes with opening 50–350 nm were used as the detecting instrument. This method provides a direct, fast and cost-effective way to characterize inorganic and organic nanoparticles in a solution.

1. Introduction

Size plays an important role in the properties of nanoparticles [1,2]. The ability to determine the size distribution and concentration of nanoparticles are extremely useful in numerous applications [3,4]. Traditionally, determination of the size and concentration of nanoparticles has been performed through chromatography [5], gel

* Corresponding author. +1 407 823 2333; fax: +1 407 823 5112.
E-mail addresses: Lee.Chow@ucf.edu, chowucf@gmail.com (L. Chow).

http://dx.doi.org/10.1016/j.colsurfa.2014.01.080
0927-7757/

electrophoresis [6], or dynamic light scattering [7]. In addition to the above methods, the Coulter counter technique [8] also has been widely used for particle counting and sensing [9,10]. The counter uses a membrane with a single tiny pore to separate chambers, filled with particle-laden solution. The ionic current through the pore, created by electric potential applied between the two chambers, depends on the diameter of the pore and drops when it is blocked by the translocation of particles. By monitoring these signals it is possible to count the number of particles translocated through the pore from one chamber to another, and the particle size can be determined if the pore size is known. The size of particle which can be detected by this method is limited by diameter of the pore. Currently, commercially available Coulter counters have a sensing pore size about a few micrometers in diameter and can detect particles as low as several hundred nanometers. Recently, several research groups used solid-state nanopores [11,12] and biological membranes [13,14] which has a size of only few nanometers. Several groups used carbon nanotubes (CNT) as a nanopore, which has a diameter as low as ~1 nm, making it ideal for DNA sensing [15,16].

Glass pipettes have several advantages over other type of pores, since they are relatively inexpensive and can be prepared with a one step procedure. Depending on the different pulling conditions such as temperature, glass thickness, and pulling force, pipette diameters down to 37 nm can be achieved [17].

In this article, we demonstrate voltage controlled translocations of SiO_2 nanoparticles and liposomes, with diameters of 80 nm to 180 nm through different size glass pipettes. In addition to the resistive pulse method, we also used ImageJ software, which retrieves particle sizes from SEM images to verify our size measurements. We notice the dependence of particle concentration on signal frequency during translocations, which increases with the concentration of nanoparticles.

2. Materials and methods

In the translocation experiments, SiO_2 nanoparticles with average diameters of 80 and 180 nm (Fig. 1(a)) and liposomes with average diameter of 100 nm were used. The SiO_2 nanoparticles were purchased from Corpuscular Inc., Cold Springs, NY, while the liposomes were prepared using lipids from Avanti Polar Lipids Inc. with the composition of 52.5% POPC (1-palmitoyl-2-oleoyl-sn-glycero-3-phosphocholine), 21% POPE (1-Palmitoyl-2-oleoyl-sn-glycero-3-phosphoethanolamine), 13% POPI (1-palmitoyl-2-oleoyl-sn-glycero-3-phospho-(1′-myo-inositol) (ammonium salt)), 3.5% POPG (1-palmitoyl-2-oleoyl-sn-glycero-3-phospho-(1′-rac-glycerol)) and 10% cholesterol. These lipids are first dissolved in chloroform (CH_3Cl) for thorough mixing. Then the chloroform is dried by steady dry nitrogen gas flow, leaving the mixed lipids formed as a film at the bottom of the vial. This vial is again placed in a vacuum pump overnight for complete drying. Finally, the hydration of lipids are realized by adding 0.5 M KCl solution and shaking vigorously. The lipids will self close to form large vesicles once hydrated, due to the hydrophobic nature of the lipid tail and hydrophilic lipid head. The desirable size of liposomes is achieved by using an extruder with 100 nm filter, (Avanti Polar Lipids Inc extrusion module and polycarbonate membranes). Both SiO_2 nanoparticles and liposomes are typically negatively charged, and the amount of charge depends on the pH value of the solution in which they have been immersed.

Micropipettes with nanopores were fabricated from borosilicate capillaries with initial inner diameter 0.8 mm and outer diameter 1.5 mm. These capillaries were placed into a pipette puller (P-2000, "Sutter, Novato", CA) in order to achieve required orifice sizes. Prior to pulling, the glass pipettes were cleaned thoroughly with alcohol.

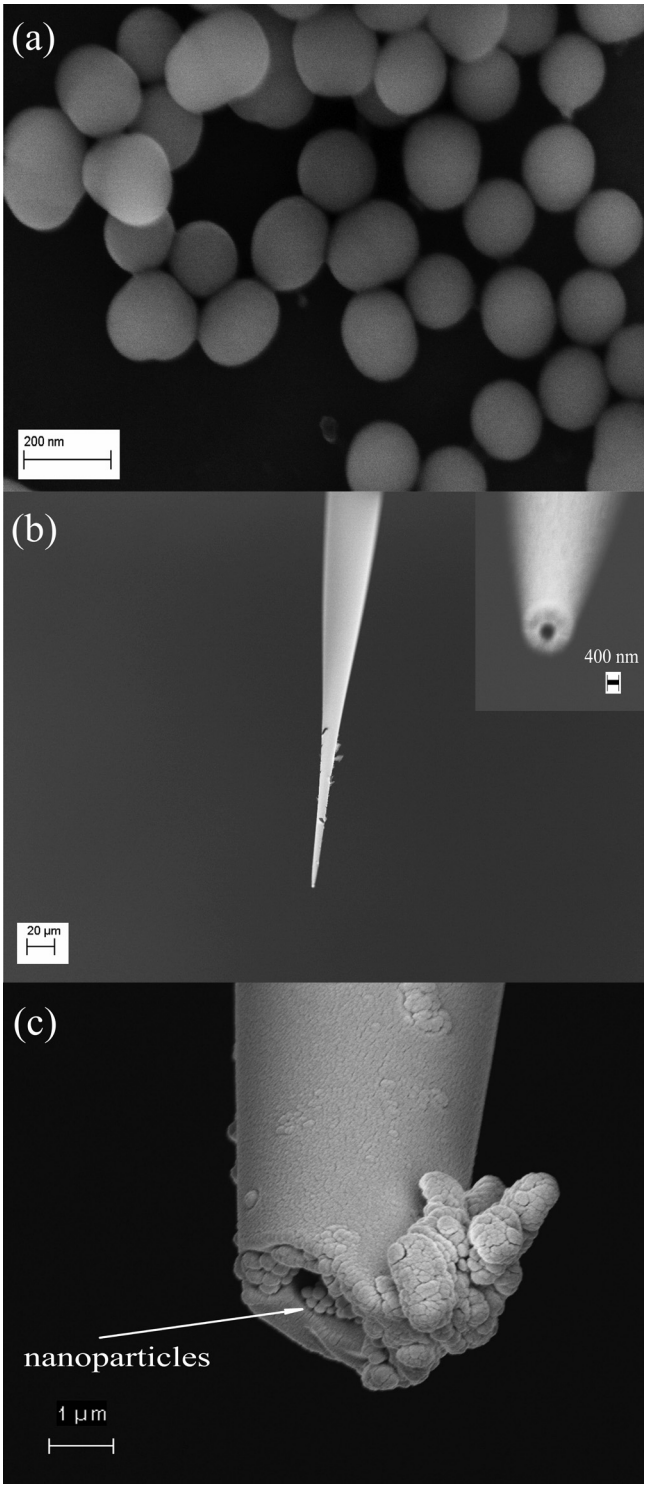

Fig. 1. (a) Silicon oxide nanospheres with average diameter 180 nm. The image was taken with Zeiss Ultra SEM. (b) Borosilicate glass capillary with a pore diameter at orifice around 320 nm (inset) (c) Image of the nanopipette with a broken tip, indicating presence of nanoparticles inside the capillary after the translocation experiment.

The inner diameters of the nanopores were determined by scanning electron microscopy (SEM) images (Fig. 1(b)) taken by *Zeiss Ultra* SEM. To prevent charging effect, these pipette tips were sputter-coated with thin platinum film before imaging.

The micropipettes with nanopores were filled with 0.1 M to 1.0 M potassium chloride (KCl) solution and immersed in the bath

with the same solution. A 0.2 mm diameter, Ag/AgCl measurement electrode was embedded into the capillary. Another Ag/AgCl reference electrode was immersed in the bath close to the micropipette tip. The average distance between electrodes was 5–7 mm. Before each experiment the electrode offset was set to zero, and ionic current was measured for different voltages. As expected the typical current–voltage (*I–V*) dependences were linear. The measured slopes of the *I–V* curves are correlated with the diameter of the pores as shown in Fig. S2. Pipettes with highly non-linear *I–V* curves, indicating broken tip, were discarded and were not used in further experiments. Afterwards, the SiO_2 nanoparticles were injected into the bath solution close to the orifice of the nanocapillary. For ionic current recording we used an Axopatch 200B amplifier in the voltage clamp mode with a low-pass Bessel filter at 2 or 5 kHz bandwidth. The signal was digitized by an Axon Instruments Digidata 1440A Series with sampling rate 250 kHz, and recorded by AxoScope 10.2 (Axon Instruments, USA). Histograms and statistical analysis were performed using Origin 8 (OriginLab, Northhampton, MA). To determine the event amplitude and duration, the base line current was calculated as an average of ionic current a few milliseconds before the event started. The difference between base line and peak current is defined as event amplitude. The moment when the current drops below a threshold is considered as the beginning of the event and vice versa for the end of the signal.

3. Results and discussions

Fig. 1(a) shows silica nanospheres with average diameter of about 180 nm used for translocations. Fig. 1(b) demonstrates the borosilicate glass capillary with a pore diameter at orifice around 320 nm (insert). Fig. 1(c) shows image of a used micropipette, clearly indicating presence of nanoparticles inside the capillary after the translocation experiment. The current-voltage (*I–V*) characteristic was checked every time before introducing nanoparticles to the translocation system. From each linear *I–V* curve, we calculate the resistance of the pore. The relationship between the resistance and the pore size was determined experimentally, using SEM images (Supplemental Fig. S2). In order to minimize the noise, the experiment set up was placed inside a Faraday cage on a vibration-isolated table. In general, noise can arise from many sources, such as a broken pipette, an ill-prepared electrode, video monitors, power lines, fluorescent lights, or mechanical vibration. In our case, the typical root-mean-square (rms) noise at 2 kHz bandwidth is in the range of 5–10 pA.

Fig. 2(a) presents current–time (*I–t*) data for translocations of SiO_2 nanoparticles (diameter = 180 nm) in 0.1 M KCl solution but with different concentrations of SiO_2 nanoparticles as indicated. Individual pulses are detected in the *I–t* trace, corresponding to the translocation of nanoparticles through the nanopore channel. At 10^{10} particles per milliliter, only two events are registered during a 10 s interval. However, as the particle concentration increased 10-fold, the translocation events seem to increase more than 10-fold. In addition, a few events with larger amplitude are also detected, as shown in Fig. 2(a). These larger pulses could be due to the translocation of aggregated nanoparticle or they can be due to the simultaneous translocation of multiple nanoparticles, resulting in relatively large amplitude with longer time duration for translocation [18–20]. Also, the frequency of current pulses increases with increasing nanoparticle concentration in solution. The event frequency also increases with the applied voltage, since stronger electrophoretic force seem to drive more particles into the nanopore [21,22]. After turning off the voltage, the translocation events were not observed. We noticed that the baseline of the 10^{12} particles per ml

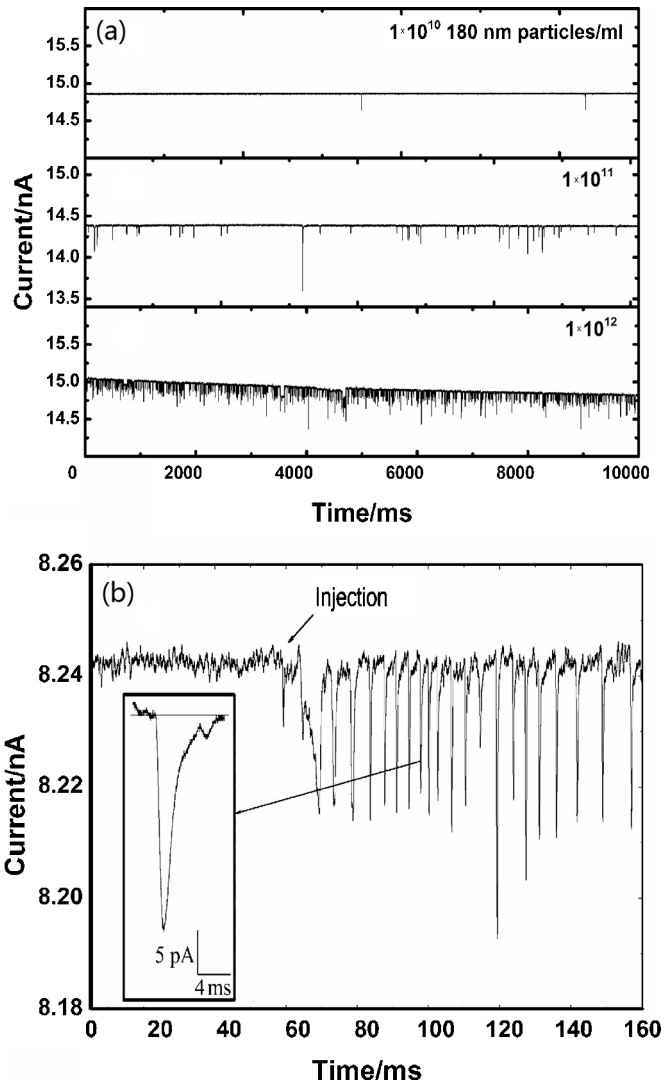

Fig. 2. (a) Translocation signals of 180 nm SiO_2 nanoparticles for three different particle concentrations: 1×10^{10} particles per milliliter, 1×10^{11} particles per milliliter, 1×10^{12} particles per milliliter. Particles were dispersed in 0.1 M KCl solution. Pipette with 320 nm pore diameter was used, and 1000 mV voltage applied. (b) Current recorded in KCl solution with SiO_2 particles injected with syringe right next to the capillary tip.

concentration is slowly decaying. This baseline current decay may be attributed to several factors such as charging effect, electrode erosion, electrochemical reactions at capillary surface and others. It requires additional investigation to verify the mechanism of this phenomenon. However, in our present work, this small base current drift will have little effect on our size calculation.

The translocated particles are clearly visible on the SEM image of nanopipette with a broken tip (Fig. 1c). According to Lan [23], the translocation of nanoparticles is driven by the electrophoretic force imposed by the applied voltage between the Ag/AgCl electrodes. In our apparatus, a resistive pulse in the *I–t* data recordings are detected as the nanoparticle passes through the orifice of the nanopore in micropipette. The average time for translocation of a 180-nm-diameter particle through our micropipette nanopore is about 4 ms at 700 mV, based on an average of 200 events.

The translocation experiment relies upon the ratio of the pore volume to the particle volume. When a particle enters a cylindrical pore the resistance *R* increases by ΔR. For the case

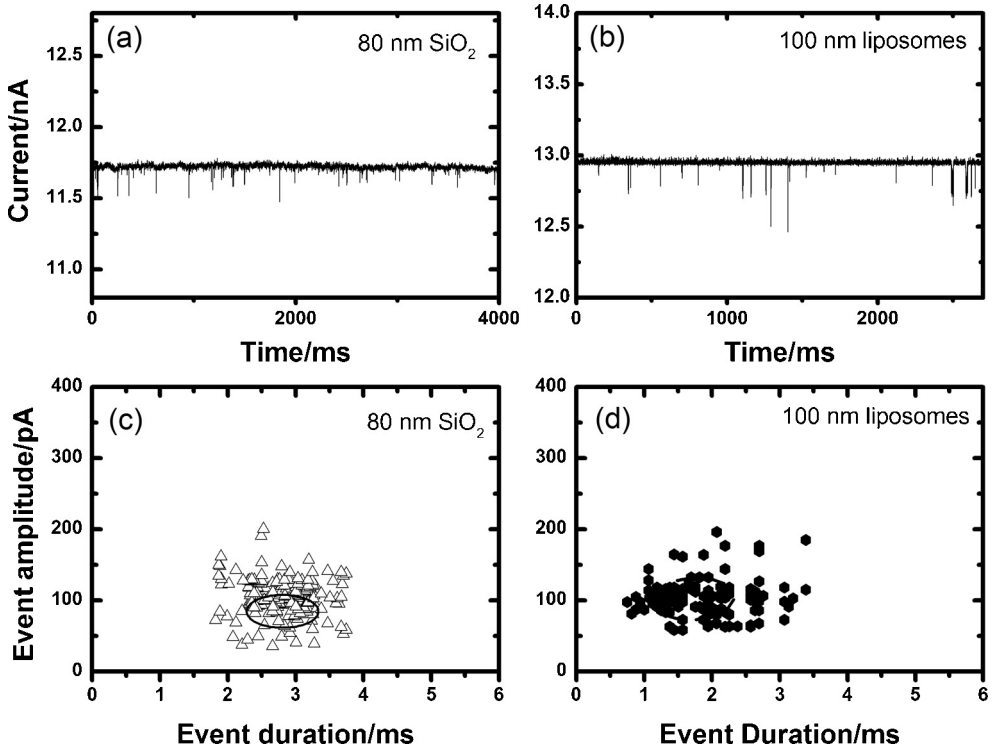

Fig. 3. (a) Translocation signals of 80 nm SiO_2 nanoparticles in 1 M KCl solution with 1000 mV potential and pore diameter 130 nm, (b) translocation signals of 100 nm vesicles in 0.5 M KCl solution with 1000 mV potential and pore diameter 160 nm, (c) event amplitude versus event duration for 171 translocation events presented on (a) and (d) event amplitude versus event duration for 140 translocation events presented on (b).

when $d < D$ and $D \ll L$, Deblois and Bean [24] presented an equation derived from the solution of a Laplace equation, which is given by,

$$\Delta R = \frac{4\rho d^3}{\pi D^4} F \tag{1}$$

where ρ is the resistivity of the solution, d is the diameter of the particle, D is the diameter of the pore, and F is a correction factor which is given by

$$F \cong 1 + 1.26\left(\frac{d}{D}\right)^3 + 1.1\left(\frac{d}{D}\right)^6 + \cdots \tag{2}$$

Since the pore resistance R is much larger than any other resistances in the circuit (electrode/fluid interfacial resistance for example), the change in current is dominated by the partial blocking of the channel. Under this condition, the relative change in resistance $\Delta R/R$ can be expressed as follows [25],

$$\frac{\Delta R}{R} = \frac{\Delta I}{I} \tag{3}$$

Combining equations (1) with (3), we end up with the following expression that related our translocation measurements to the size of particles:

$$d = \sqrt[3]{\frac{\Delta I V \pi D^4}{4\rho I^2 F}} \tag{4}$$

where ΔI is the change in current, I is the background current, and other parameters in this equation have been given in previous paragraphs. We note that Eq. (4) is independent of the length of the channel L. With this equation, all translocation measurements of particle size using different pore size can be plotted in one graph.

One approximation in this model is that the conduction channel is considered to be a cylindrical channel, which is a simplified version of the conical shape channel of the glass pipette. Asymmetry of the channel affects two aspects of the resistive pulse measurements: (a) the slow increase of the current as the particle goes gradually toward larger radius part of the pipette, (b) net resistance of the channel. However, it has no consequence on our measurements, since we only use the maximum pulse height for our size measurement [26]. The net resistance of the asymmetrical channel is already reflected in the base current (corresponding to an open pore). We demonstrate later that this simple model yields very good agreement with the data obtained from direct imaging of the nanoparticles.

In Fig. 2(b) we showed a typical current vs. time translocation plot of SiO_2 nanoparticles through a 320 nm pore opening into the micropipettes. The solution used here is 0.1 M KCl and the SiO_2 nanoparticles have a diameter of 180 nm. As we can see that before the injection of the SiO_2 nanoparticles, the ionic current is rather stable with a fluctuation of about ~2 pA. After the injection of the nanoparticles, the sudden change of the current (blockage of current) is caused by the translocation of the nanoparticles through the micropipette channel. The maximum amplitude occurred at the point where the channel has a minimum dimension, i.e. at the tip of the micropipettes. The typical amplitude of current blockage is about 50–200 pA and the frequency of blockages in this particular case is around 250 ± 50 Hz, which mostly depends on the concentration of the nanoparticles and to a lesser degree also on the applied voltage used. The insert in Fig. 2(b) showed an enlarged view of a single translocation event. We can see that the current dropped abruptly (within 1.5 ms), from the background current value to its minimum value before it gradual recover its background current within 2–3 ms. This signal behavior is commonly observed in other similar translocation experiments [18,23,27] when a conical shaped channel is used.

Next we demonstrate that the micropipette-based resistive pulse method can be used for smaller SiO_2 nanoparticles and also

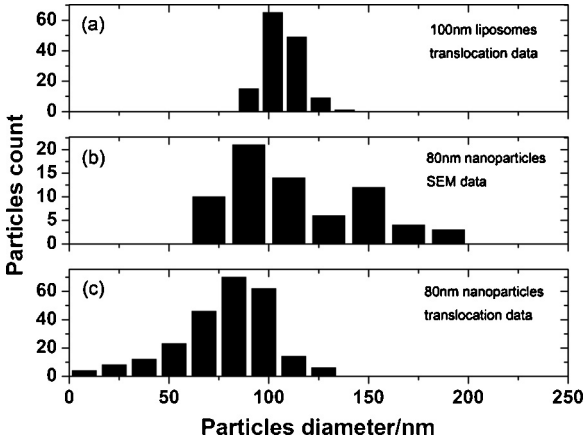

Fig. 4. (a) Size distribution of 100 nm liposomes from translocation data, (b) size distribution of 80 nm SiO_2 nanoparticles obtained by analyzing SEM image, (c) size distribution of 80 nm SiO_2 nanoparticles from translocation data.

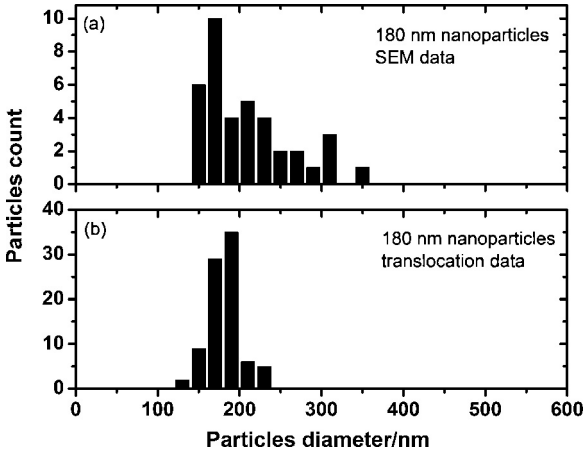

Fig. 5. (a) Size distribution of 180 nm SiO_2 nanoparticles obtained by analyzing SEM image, (b) Size distribution of 80 nm SiO_2 nanoparticles obtained by using experimental translocation data.

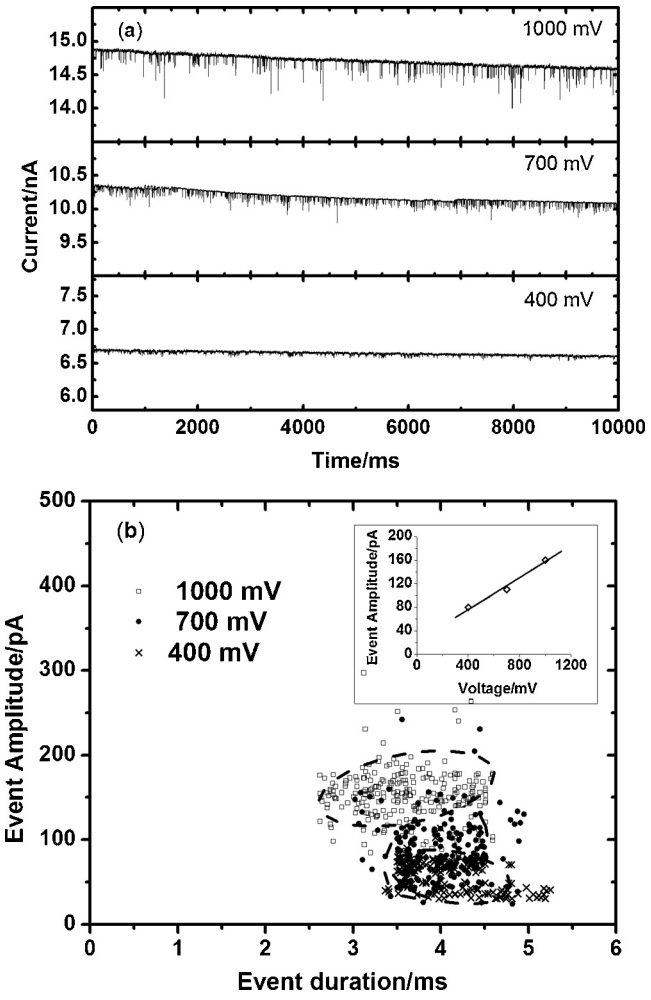

Fig. 6. (a) Translocation signals of 180 nm SiO_2 nanoparticles for three different voltage: (a) 1000 mV potential, (b) 700 mV potential, (c) 400 mV potential. Particles were dispersed in 0.1 M KCl solution. Pipette with 320 nm pore diameter was used (b) event amplitude versus event duration plot for three different voltages: 1000 mV, 700 mV, 400 mV and dependence of event amplitude versus voltage (see inset).

for synthesized artificial vesicles such as liposomes. Fig. 3(a) shows the translocation events of 80 nm SiO_2 nanoparticles in 1 M KCl solution with 1.0 V potential applied. The pore diameter of the pipette in this case is 120 nm. Fig. 3(b) shows the translocation events of 100 nm diameter liposomes in 0.5 M KCl solution. The potential applied is 1.0 V and a 160 nm pore micropipette is used in this case. The baseline current represents the ionic conduction through the nanopore when no translocation occurs. In Fig. 3(a) and (b), baseline currents of 11.7 nA and 13.0 nA are obtained. In Fig. 3(c) and (d), event amplitudes versus event duration of the translocations peaks are presented as scatter plots. Fig. 3(c), shows scatter plot for the 80 nm SiO_2 nanoparticles, while Fig. 3(d) shows translocation events of 100 nm vesicle particles. In both cases, we can see that each translocation event is represented as one data point in the scatter plots. Using the event current obtained from the scatter plots and the Eq. (4) above, we are able to plot the size distribution of the nanoparticles independent of the size of the nanopore used or the applied voltage across the nanopore. Note that we use different KCl concentrations for the above measurements to demonstrate that the technique is applicable in a broad range of KCl concentrations.

In Fig. 4, the size distributions of 100 nm vesicles and 80 nm SiO_2 nanopartcles are shown together with the size distribution of 80 nm SiO_2 nanoparticles obtained from SEM images analyzed with ImageJ software. Fig. 5 shows size distribution of 180 nm SiO_2 nanoparticles. We can see that the SEM image analysis data showed a long tail at larger size, while the translocation data showed a slightly longer tail at the smaller size. This is understandable and is due to the intrinsic property of the techniques. Namely the translocation method seems to favor smaller particles since it will block all particles which are larger than the pore size, while the image method tends to favor larger particles. Otherwise, there is reasonable agreement between the translocation data and the SEM analysis of the 80 nm and 180 nm SiO_2 nanoparticles, since both indicate the maximum distribution at around 80 nm and 180 nm, respectively. The vesicle size distribution presented in Fig. 4(a) showed a narrower distribution.

We also investigated the influence of electrode voltage on the translocation of nanoparticles. In Fig. 6(a), the translocation plots of 180 nm SiO_2 particles in 0.1 M KCl solution are shown with electrode voltages of 1000 mV, 700 mV, and 400 mV, respectively. In Fig. 6(b), cluster plots of the three translocations at different voltages are shown. The differences between translocation processes at different voltages are evident. When 1000 mV applied to the electrode, the current pulses are easily observed. The average amplitude of the current pulses are on the order of 150 pA which can be seen in Fig. 6(b). However, we do observe a few relatively large pulses, which could be due to aggregated nanoparticles. Decreasing voltage from 1000 mV to 700 mV demonstrates a reduction in the

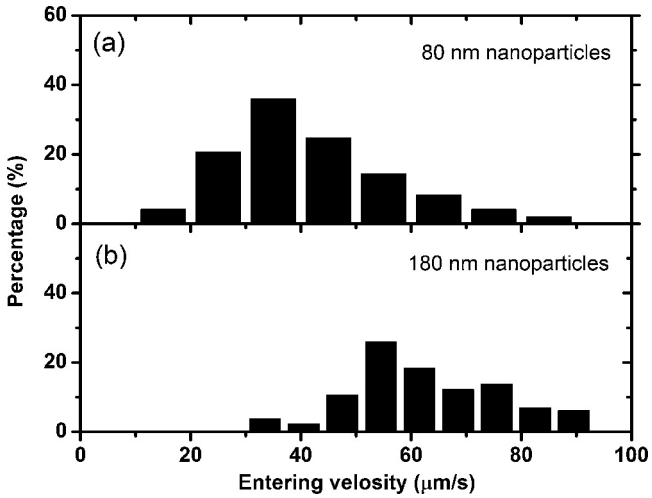

Fig. 7. Average entering velocity distribution for (a) 80 nm (top) and (b) 180 nm (bottom) SiO_2 nanoparticles.

event amplitude and an increase in the event duration (Fig. 6(b)). With a further decreasing of applied voltage to 400 mV, the average event amplitudes are further reduced to below 100 pA. In the insert of Fig. 6(b), we show the average event amplitudes of three translocation events. It can be seen that the event amplitudes are almost linearly proportional to the applied electrode voltage as the previously described theory would predict.

In the translocation measurements, we measure both the event amplitude and the event duration. The event amplitude is related to the size of the nanoparticles as we discussed earlier. Here we will pay some attention to the event duration. The event duration typically depends on (a) the velocity of the nanoparticles, and (b) the length of the channel. For a tapered channel such as a pulled pipette, it is difficult to define the exact length of the channel. Here we will examine the translocation pulse shape in the insert of Fig. 2(b) and propose to use the leading edge of the current pulse to define an entry time. We define the entry time as the time interval required for the base line current to drop to its minimum value in a single translocation signal. This time interval is associated with the time required for a particle to travel a distance of its radius as it enters the micropipette.

Using this methodology, we analyze the average entering velocity of two different size SiO_2 particles of 80 nm and 180 nm. The average entering velocity is assumed to be the ratio of radius to entering time for each particle. In Fig. 7 the distributions of the entering velocity for 80 nm and for 180 nm SiO_2 nanoparticles are shown. In both cases, the electrode voltage was 1.0 V, and particles were dispersed in KCl bath solution with the same pH value. Our results showed that the average velocity of 80 nm SiO_2 nanoparticle is about 36 μm/s, while the 180 nm SiO_2 nanoparticle has an average velocity of 60 μm/s.

The terminal velocity of a nanoparticle in a fluid will depend on the size of the nanoparticle, the amount of charge it carries, the potential difference between the two electrodes, and the viscosity of the fluid. Comparing with size measurements, velocity measurements of nanoparticles are usually more difficult. Currently, several techniques used for nanoparticles velocity determination. For example, micro electrical field flow fractionation has been used [28] to measure the velocity of fluorescent nanoparticles. They found that 28 nm size polymer nanospheres have an average velocity of 50 μm/s. However, most widely used methods, which simultaneously can measure particle size and velocity, are dynamic light scattering [29,30] and laser doppler velocimetry [31]. Judging from these previously published data, our preliminary velocity measurements seem to be reasonable. Our technique, as an alternative, is more accessible and may work with smaller nanoparticle size. Finally we want to point out that the sample size of this resistive pulse method can be made quite small. In our case, a droplet of volume below 1 μl has been used for some translocation measurements presented here.

4. Conclusion

In this study, we successfully demonstrated a simple "resistive-pulse" method based on micropipettes that allow us to observe translocations of nanoparticles, counting and measuring size and velocity distribution of inorganic and organic nanoparticles. The method permits us to precisely measure the size of nanoparticles in a size range from 50 nm to 250 nm in diameter in the solution, as well as to measure their velocity and to analyze its concentrations. One major advantage of the resistive pulse method is the potential to use relatively minute sample size. The resistive pulse method could have significant applications in a number of fields ranging from sensing nanoparticles, drug delivery, nanoparticles counting, because it provides a direct, fast and accessible way to characterize nanoparticles in a solution.

Acknowledgement

LC acknowledges the financial support of National Science Foundation through Grant ECCS 0901361. The authors also thank Dr. S. Tatulian and Dr. K. Nemec for the assistance in liposome preparation.

Appendix A. Supplementary data

Supplementary material related to this article can be found, in the online version, at http://dx.doi.org/10.1016/j.colsurfa.2014.01.080.

References

[1] Ph. Buffat, J.-P. Borel, Size effect on the melting temperature of gold particles, Physical Review A 13 (1976) 2287–2298.
[2] V.I. Klimov, A.A. Mihhailovsky, S. Xu, A. Malko, J.A. Hollingsworth, C.A. Leatherdale, A. Eisler, M.G. Bawendi, Optical gain and stimulated emission in nanocrystal quantum dots, Science 290 (2000) 314–317.
[3] V.L. Colvin, M.C. Schlamp, Allvisatos, Light-emitting diodes made from cadmium selenide nanocrystals and a semiconducting polymer, Nature 370 (1994) 354–357.
[4] G. Oberdorster, E. Oberdorster, J. Oberdorster, Nanotoxicology: an emerging discipline evolving from studies of ultrafine particles, Environmental Health Perspectives 113 (2005) 823–839.
[5] A. Striegel, W.W. Yau, J.J. Kirkland, D.D. Bly, Modern Size-Exclusion Liquid Chromatography: Practice of Gel Permeation and Gel Filtration Chromatography, second ed., 2009.
[6] B. Alberts, D. Bray, J. Lewis, M. Raff, K. Roberts, J.D. Watson, Molecular Biology of the Cell, Garland, New York, NY, 1994.
[7] W.B. Russel, D.A. Saville, W.R. Schowalter, Colloidal Dispersions, Cambridge University Press, New York, NY, 1989.
[8] W.H. Coulter, U.S. Patent No. 2,656,508, 1953.
[9] J. Hurley, Sizing particles with a Coulter counter, Biophysical Journal 10 (1) (1970) 74–79.
[10] J. Zhe, A. Jagtiani, P. Dutta, J. Hu, J. Carletta, A micromachined high throughput Coulter counter for bioparticle detection and counting, Journal of Micromechanics and Microengineering 17 (2007) 304–313.
[11] C. Dekker, Solid-state nanopores, Nature Nanotechnology 2 (4) (2007) 209–215.
[12] J. Gao, W. Guo, H. Geng, X. Hou, Z. Shuai, L. Jiang, Layer-by-layer removal of insulating few-layer mica flakes for asymmetric ultra-thin nanopore fabrication, Nano Research 5 (2) (2012) 99–108.
[13] S.M. Bezrukov, Ion channels as molecular Coulter counters to probe metabolite transport, Journal of Membrane Biology 174 (1) (2000) 1–13.
[14] A. Meller, D. Branton, Single molecule measurements of DNA transport through a nanopore, Electrophoresis 23 (2002) 2583–2591.
[15] H. Liu, J. He, J. Tang, H. Liu, P. Pang, D. Cao, P. Krstic, S. Joseph, S. Lindsay, C. Nuckolls, Translocation of single-stranded DNA through single-walled carbon nanotubes, Science 327 (2010) 64–67.

[16] T. Ito, L. Sun, R.R. Henriquez, R.M. Crooks, A Carbon nanotube-based Coulter nanoparticle counter, Accounts of Chemical Research 37 (2004) 937–945.
[17] M. Karhanek, J.T. Kemp, N. Pourmand, R.W. Davis, C.D. Webb, Single DNA molecule detection using nanopipettes and nanoparticles, Nano Letters 5 (2) (2005) 403–407.
[18] W.J. Lan, D.A. Holden, B. Zhang, H.S. White, Nanoparticle transport in conical-shaped nanopores, Analytical Chemistry 83 (2011) 3840–3847.
[19] M.M. Figueiredo, in: R.A. Meyers (Ed.), Encyclopedia of Analytical Chemistry, John Wiley & Sons, New York, NY, 2000, pp. 5358–5371.
[20] D.A. Holden, G. Hendrickson, L.A. Lyon, H.S. White, Resistive pulse analysis of microgel deformation during nanopore translocation, Journal of Physical Chemistry C 115 (2011) 2999–3004.
[21] L. Bacri, A.G. Oukhaled, B. Schiedt, G. Patriarche, E. Bourhis, J. Gierak, J. Pelta, L. Auvray, Dynamics of colloids in single solid-state nanopores, Journal of Physical Chemistry B 115 (2011) 2890–2898.
[22] R. Chein, P. Dutta, Effect of charged membrane on the particle motion through a nanopore, Colloids and Surfaces A: Physicochemical and Engineering Aspects 341 (2009) 1–12.
[23] W.J. Lan, D.A. Holden, H.S. White, Pressure-dependent ion current rectification in conical-shaped glass nanopores, Journal of the American Chemical Society 133 (2011) 13300–13303.
[24] R.W. Deblois, C.P. Bean, Counting and sizing of submicron particles by the resistive pulse technique, Review of Scientific Instruments 41 (7) (1970) 909–915.
[25] O.A. Saleh, L.L. Sohn, Quantitative sensing of nanoscale colloids using a microchip Coulter counter, Review of Scientific Instruments 72 (12) (2001) 4449–4451.
[26] G. Stober, L.J. Steinbock, U.F. Keyser, Modeling of colloidal transport in capillaries, Journal of Applied Physics 105 (2009) 084702.
[27] L.J. Steinbook, G. Stober, U.F. Keyser, Sensing DNA-coatings of microparticles using micropipettes, Biosensor and Bioelectronics 24 (2009) 2423–2427.
[28] M.-H. Chang, D. Dosev, I.M. Kennedy, Zeta-potential analyses using micro electrical field flow fractionation with fluorescent nanoparticles, Sensors and Actuators B Chemistry 124 (1) (2007) 172–178.
[29] B.A. Leung, K.I. Suh, R.R. Ansari, Particle-size and velocity measurements in flowing conditions using dynamic light scattering, Applied Optics 45 (10) (2006) 2186–2190.
[30] T. Ito, L. Sun, M.A. Bevan, R.M. Crooks, Comparison of nanoparticle size and electrophoretic mobility measurements using a carbon-nanotube-based Coulter counter, dynamic light scattering, transmission electron microscopy, and phase analysis light scattering, Langmuir 20 (2004) 6940–6945.
[31] B. Xiong, A. Pallandre, I. Potier, P. Audebert, E. Fattal, N. Tsapis, G. Barratt, M. Taverna, Electrophoretic mobility measurement by laser Doppler velocimetry and capillary electrophoresis of micrometric fluorescent polystyrene beads, Analytical Methods 4 (2012) 183–189.